RSC Advances

PAPER

View Article Online
View Journal | View Issue

Cite this: *RSC Adv.*, 2019, **9**, 40131

Glycyrrhetinic acid modified and pH-sensitive mixed micelles improve the anticancer effect of curcumin in hepatoma carcinoma cells

Jizheng Song, †[a] Yuling Liu, †[a] Longfei Lin, [a] Ye Zhao,[a] Xiuqing Wang,[a] Ming Zhong,[b] Tanggui Xie,[b] Yuting Luo,[a] Shaojing Li,[a] Ruocong Yang[a] and Hui Li*[a]

Received 10th September 2019
Accepted 27th November 2019

DOI: 10.1039/c9ra07250k

rsc.li/rsc-advances

Curcumin (CUR), a natural polyphenolic compound existing in plants, exhibits anticancer potential in inhibiting the growth of various types of human cancer. However, the poor aqueous solubility and low bioavailability limit its clinical applications. pH-sensitive macromolecule F68-acetal-PCL (FAP) and active targeting macromolecule F68-glycyrrhetinic acid (FGA) were designed to fabricate mixed micelles for efficient delivery of CUR. The thin film hydration method was used to prepare CUR loaded mixed (MIX/CUR) micelles. The drug loading rate (DL) of MIX/CUR micelles was 6.31 ± 0.92%, which remained stable for 15 days at 4 °C. The particle size and zeta potential of the MIX/CUR micelles were 91.06 ± 1.37 nm and −9.79 ± 0.47 mV, respectively. The MIX/CUR micelles exhibited pH sensitivity in a weak acid environment, and showed rapid particle size variation and drug release. In addition, *in vitro* tests demonstrated that MIX/CUR micelles induced higher cytotoxicity and apoptosis than free CUR, non-pH-sensitive F68-PCL (FBP)/CUR micelles and pH-sensitive FAP/CUR micelles in SMMC7721 and Hepa1-6 cells. Besides, mixed micelles were more effective than FBP and FAP micelles in a cell uptake experiment, which was medicated by a GA receptor. All in all, these results indicated that MIX/CUR micelles could be regarded as an ideal drug administration strategy against hepatoma carcinoma cells.

1 Introduction

Hepatoma, a common malignant disease, is the second leading cause of cancer-associated death worldwide.[1–3] Curcumin (CUR) is included in the FDA GRAS (generally regarded as safe) list, and inhibits the growth of different types of cancer without obvious side effects.[4–11] Modern research suggests that CUR exerts anticancer effects through various mechanisms which play essential roles in the development and progression of cancer.[12–14] The mechanisms include different types of cytokines, enzymes and growth factors, such as MAPK, NF-κB, COX-2, STAT3 and TNF-α. Nevertheless, the challenges of CUR including poor aqueous solubility, and low bioavailability and photo-labile properties should be overcome before clinical application.[15]

Nanotechnology has been employed to design varies drug delivery systems including polymer micelles, nanoparticles, liposomes, *etc.*, which showed great potential in improving the therapeutic effects and overcoming the shortages of CUR.[16] Among these strategies, polymer micelles as one of nano drug delivery systems that has been used to improve the stability, water solubility, and cancer proliferation inhibition of CUR.[17–19] Pluronic F68, a widely used amphiphilic triblock polymer in drug delivery, which was approved by the FDA for intravenous injection.[20] However, the high critical micelle concentration (CMC) of F68 might led to disaggregation in circulation systems.[21,22] In order to improve the amphiphilic property of F68, polycaprolactone (PCL) was grafted with F68 to establish drug carrier owing to its hydrophobicity.[20,23–28] In previous reports, CUR loaded polymer micelles might face ineffective drug release problems in tumor tissues or cells.[4] So as to achieve rapid intracellular drug release, the acid sensitive linkage between hydrophobic group and hydrophilic group could be employed to hydrolyze rapidly in weakly acid environment of tumor. Hence, acetal linkage has the ability to apply in fabricating pH-sensitive amphiphilic polymer in response to the tumor microenvironment.[29,30] In addition, glycyrrhetinic acid (GA), the receptor overexpressed on the surface of hepatoma cells, was also chosen to modify with the F68 polymer with the aim of better tumor targeting.[31–35]

Herein, CUR loaded mixed micelles (MIX/CUR) which composed of F68-acetal-PCL (FAP) and F68-GA (FGA) polymers were prepared to attain tumor targeted and acid sensitive goals in this study (Fig. 1). Among the mixed micelles, FAP polymer was the pH-sensitive polymer that bounded F68 and PCL *via* the acetal linkage. And the FGA polymer represented that F68 was esterified with GA. Firstly, FAP and FGA polymers used in the

[a]*Institute of Chinese Materia Medica, China Academy of Chinese Medical Sciences, Beijing 100700, China. E-mail: lihuizys@126.com*

[b]*Guangxi Key Laboratory of Traditional Chinese Medicine Quality Standards, Guangxi Institute of Chinese Medicine and Pharmaceutical Science, Nanning 530022, China*

† These authors contributed equally to this work.

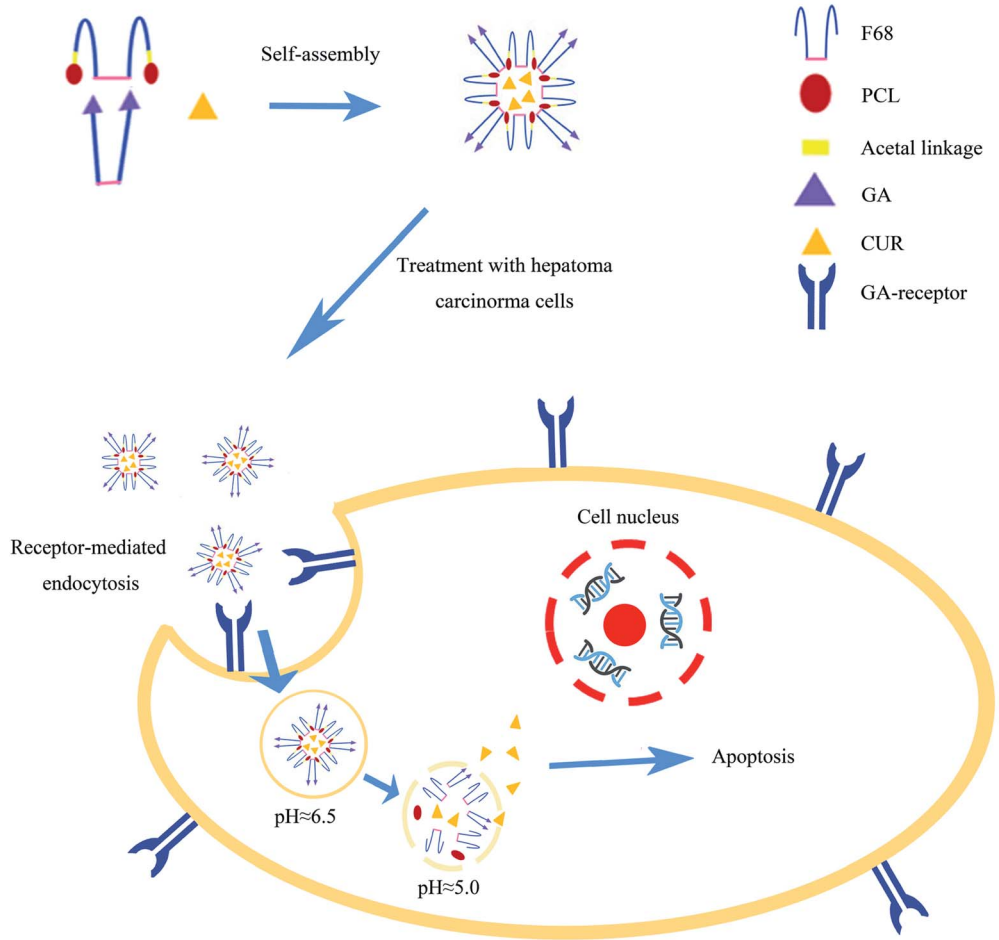

Fig. 1 The preparation of MIX/CUR micelles, receptor-mediated endocytosis and pH-responded CUR released from the micelles to increase the cellular apoptosis.

mixed micelles were synthesized and the structures were confirmed by nuclear magnetic resonance spectroscopy (^{1}H-NMR) and Fourier transform infrared spectroscopy (FTIR). Secondly, the mixed micelles were prepared and the particle sizes or zeta potentials were measured by dynamic light scattering (DLS). The encapsulation efficiency (EE) and drug loading (DL) were detected by HPLC, respectively. The stability, *in vitro* drug release behaviors and CMC of the mixed micelles were also measured. Thirdly, the mixed micelles systems showed favorable pH-sensitivity and suitable biocompatibility *in vitro*. Subsequently, *in vitro* cytotoxicity, the cellular uptake, pro-apoptotic activities and ROS assays of the MIX/CUR micelles against hepatoma carcinoma cells (HCC) were investigated. Collectively, these results showed that the newly developed dual-functional mixed micelles may be utilized to deliver CUR for anticancer therapy.

2 Materials and methods

2.1 Materials

CUR and GA were obtained from J&K. Pluronic F68 (F68, molecular weight = 8350), 1-(3-dimethylpropane)-3-ethylcarbodiimide hydrochloride (EDC·HCl), 4-dimethylaminopyridine (DMAP) and Hoechst 33342 were bought from Aladdin Industrial Corporation (Shanghai, China). Polycaprolactone (PCL) was purchased from Daigang Biomaterial Co., Ltd (Jinan, China). Ethylene glycol vinyl ether (EGVE) was purchased from Ouhe Technology Co., Ltd (Beijing, China). Triethylamine (TEA), sodium dodecyl sulfate (SDS) and *p*-toluenesulfonic acid (PTSA) were purchased from Damao Chemical Reagent Factory (Tianjin, China). All chemicals were analytical grade. Ultrapure water was prepared by Milli-Q Plus System (Merck Millipore Co., Billerica, MA, USA). 3-[4,5-Dimethyl-2-thiazolyl]-2,5-diphenyl tetrazolium bromide (MTT) was obtained from Sigma-Aldrich (St Louis, MO, USA). Fetal Bovine Serum (FBS), penicillin–streptomycin, 0.25% (w/v) trypsin/1 mM EDTA, Dulbecco's Modified Eagle's Medium (DMEM) and phosphate-buffered saline (PBS) were obtained from Gibco. Annexin V-FITC and propidium iodide (PI) were purchased from Nanjing Jiancheng Bio-engineering Institute (Nanjing, China).

2.2 Cell culture

SMMC-7721, Hepa1-6, HepG-2, and L-02 cell lines were acquired from the Library of Chinese Academy of Sciences Cells. SMMC-7721, Hepa1-6, HepG-2, and L-02 cells were cultured in

DMEM which containing 10% FBS (v/v) and antibiotics (100 mg mL^{-1} streptomycin and 100 U mL^{-1} penicillin) under 5% CO_2 at 37 °C.

2.3 Synthesis of FAP polymer

FAP polymer was synthesized with two steps. First, PCL–CH=CH_2 was synthesized by esterification. PCL (740 mg, 0.2 mmol), EGVE (27 μl, 0.3 mmol), DMAP (36.65 mg, 0.3 mmol), EDC (57.50 mg, 0.3 mmol) and TEA (42 μl, 0.3 mmol) were dissolved in 10 mL dry dichloromethane (DCM) and stirred well at room temperature. 48 h later, DCM was removed by rotary evaporation. After the residues were dissolved in acetone, the solution in dialysis bag with molecular weight cutoff (MWCO) at 3500 Da was dialyzed against water to remove unreacted materials. PCL–CH=CH_2, the intermediate produce, was obtained by freeze-drying. Second, FAP polymer was synthesized by electrophilic addition reaction. In short words, PCL–CH=CH_2 (530 mg, 0.14 mmol), PTSA (2.41 mg, 0.014 mmol) and F68–OH (588 mg, 0.07 mmol) were dissolved in 10 mL dry DCM and stirred well at room temperature. 48 h later, 4 mg K_2CO_3 was added to neutralize PTSA for terminating the reaction. After that DCM was removed by rotary evaporation, the residues were re-dissolved in acetone and dialyzed against ammonia water (pH = 9.0) in dialysis bag with MWCO at 3500 Da to remove unreacted materials. Finally, FAP was obtained by freeze-drying.

2.4 Synthesis of FGA polymer

FGA polymer was synthesized by esterification. Briefly, GA (141.2 mg, 0.3 mmol), F68 (840.0 mg, 0.1 mmol), DMAP (36.7 mg, 0.3 mmol), EDC (57.5 mg, 0.3 mmol) and TEA (31 μl, 0.3 mmol) were dissolved in 10 mL dry DCM and stirred at room temperature. 48 h later, DCM was removed by rotary evaporation, residues were resolved in acetone and dialyzed against water in dialysis bag with MWCO at 3500 Da to remove unreacted materials. At last, FGA was obtained by freeze-drying.

2.5 Characterizations of FAP and FGA conjugates

The structures of FAP and FGA polymers were identified with FTIR spectrophotometer (Frontier IR, PerkinElmer Inc., USA). The polymers and potassium bromide were mixed uniformly and pressed into a thin sheet with tableting machine (FW-4A, Tuopu instrument Co., Ltd, China) under 22 MPa. The spectra were scanned from 400 cm^{-1} to 4000 cm^{-1}. Additionally, the structures were further identified by ^{1}H-NMR (Bruker, Karlsruhe, Germany) at 600 MHz with deuterated chloroform as the solvent.

2.6 Preparation of MIX/CUR micelles and blank mixed micelles

MIX/CUR micelles were prepared by self-assembly using thin film hydration method. First, 5 mg FAP, 5 mg FGA and 1 mg CUR were completely resolved in 5 mL acetone. Acetone was removed by rotary evaporation to obtain yellow thin film in the eggplant-shaped bottle. Second, 10 mL PBS (pH = 7.4) at 60 °C was added in the eggplant-shaped bottle, then it was spun in water bath at 60 °C for 30 min. The final MIX/CUR micelles were acquired by filtering with 0.22 μm membrane. In addition, blank mixed micelles (BMM) were also prepared by the method mentioned above.

2.7 Characterization of MIX/CUR micelles

MIX/CUR micelles were analyzed with particle size, zeta potential and morphology. DLS (Malvern Instruments, Malvern, UK) was employed to detect the particle size and zeta potential of MIX/CUR micelles at room temperature. The morphology of MIX/CUR micelles was observed by transmission electron microscopy (TEM, JEM 1400 Plus, JEOL Ltd, Japan) under the accelerating voltage of 100 kV. The quality of CUR in MIX/CUR micelles was performed on C_{18} reverse-phase liquid chromatography column (250 × 4.6 mm) under the flow rate of 1 mL min^{-1} and the maximum absorption wavelength of 430 nm in Shimadzu LC-20AT HPLC. The mobile phase was methanol/0.1% phosphoric acid (75/25, v/v). The micelles were dissolved in methanol to disrupt micelle shells. The experiments were performed in triplicate. The DL and EE were calculated by the following equations:

$$\mathrm{DL}\ (\%) = M_1/(M_1 + M_2) \times 100\%$$

$$\mathrm{EE}\ (\%) = M_1/M_3 \times 100\%$$

M_1 represents the total amount of drug encapsulated in the micelles; M_2 represents the weight of polymer materials which are used for preparing the micelles. M_3 represents the dosage.

2.8 pH-responsive degradation of the micelles

In order to investigate the pH-responsive disaggregation of the micelles, the pH values of micelles were turned to 5.0 by 0.05 mol L^{-1} HCl. The solutions were incubated in a shaker with 100 rpm shaking rate at 37 °C. At predetermined intervals (0 h, 1 h, 2 h, h, 8 h, 12 h and 24 h), DLS was used to detect the pH-responsive size changes of the micelles. Morphology of pH-sensitive particle size changes was observed by TEM after 24 h. The experiments were performed in triplicate.

2.9 Determination of CMC

Firstly, the anti-dilution property of BMM was evaluated by Tyndall phenomenon. In short words, a series of concentrations of BMM ranging from 1.0×10^{-4} mg mL^{-1} to 1.0 mg mL^{-1} were diluted for the experiments. Then, laser pen was used to illuminate the solutions to observe if the micelles showed a visible light beam.

Secondly, fluorescence spectrometer was employed to determine the CMC value. In this method, pyrene was used as fluorescence probe. The concentration of BMM was varied from 1.0×10^{-6} till 1.0 mg mL^{-1} and the ultimately concentration of pyrene was 6.0×10^{-7} mol L^{-1}. The fluorescence spectra were recorded by fluorescence spectrometer (F7000, HITACHI Company, JAPAN) with the excitation wavelength at 337 nm. The emission fluorescence at 373 and 383 nm were monitored for calculation.

2.10 *In vitro* release of CUR from micelles

The release curves of CUR were investigated by a dialysis bag (MWCO 5000 Da) with 100 rpm shaking rate at 37 °C in PBS which containing 0.5% SDS with different pH (5.0 and 7.4), respectively. As a control group, CUR was solubilized in DMSO. 2 mL FAP/CUR, F68-ester bond-PCL (FBP)/CUR, MIX/CUR micelles or control solution (equivalent to 0.15 mg CUR) were dialyzed against 20 mL release media. 2 mL sample was withdrawn at predetermined time intervals (0 h, 0.5 h, 1 h, 2 h, 4 h, 8 h, 12 h, 24 h and 48 h) and swapped by fresh medium of equal volume. The concentration of CUR in the sample was determined by UV-vis (T6, Persee, China) at 430 nm. The accumulative percentage of released CUR should be calculated according to the following formulates. The release experiments were performed in triplicate.

$$M_t = C_i \times 20\ \text{mL} + \sum_{i=1}^{n-1} C_i \times 2\ \text{mL}$$

$$\text{Accumulative release rate (\%)} = (M_t/M_i) \times 100\%$$

M_t represents the total amount of released drug at the interval time point; C_i (mg mL^{-1}) represents the CUR concentration in medium at the interval time point; $\sum_{i=1}^{n-1} C_i \times 2$ mL represents the total amount of released drug until the i^{th} time point; M_i represents the initial amount of CUR in the dialysis bag.

2.11 The stability of MIX/CUR micelles

The particle size and zeta potential in 15 days were measured to characterize the stability of MIX/CUR micelles. The micelles were stored at 4 °C and measured by DLS at room temperature.

Besides, the stability of MIX/CUR micelles was also investigated in PBS contained 10% FBS, which could simulate the condition of circulation system. Briefly, MIX/CUR micelles were exposed to PBS contained 10% FBS and incubated at 37 °C. At different predetermined time intervals (0 h, 4 h, 8 h, 12 h, 24 h), the particle size of MIX/CUR micelles was measured by DLS.

2.12 Hemolysis assay

The previous method was used to evaluate the hemolysis of BMM.[36] To separate red blood cells (RBCs) from fresh rat blood, the blood was combined with heparin sodium physiological saline solution (1000 U mL^{-1}) and centrifuged at 1500 rpm for 20 min. Physiological saline was employed to wash the RBCs for three times. Then, physiological saline was used to dilute the RBCs for obtain 2% (v/v) erythrocyte suspension. BMM were diluted with physiological saline at various concentrations, then equal volume of erythrocyte suspension was added in it. The mixtures were shook in 100 rpm at 37 °C for 3 h, then the mixtures were centrifuged at 1500 rpm for 20 min. The supernatant liquid was measured by microplate reader (SpectraMax M5, Molecular Devices LLC, USA) at 540 nm. Physiological saline and distilled water were set as the negative and positive controls, respectively. All hemolysis experiments were performed in triplicate. The following equation was used to calculate the hemolysis rate of each groups:

$$\text{Hemolysis rate (\%)} = (A_s - A_n)/(A_p - A_n) \times 100\%$$

A_s, A_n, and A_p represented the absorbance of samples, negative control and positive control at 540 nm, respectively.

2.13 Cytotoxicity assay

MTT assay was employed to measure the *in vitro* cytotoxicity of FAP/CUR, MIX/CUR, FBP/CUR, blank FAP, blank mixed and blank FBP micelles against SMMC-7721, Hepa1-6, HepG-2, and L-02 cells. They (8000 per well) were placed in 96-well plate in 100 μL DMEM medium which containing 10% FBS. After incubation overnight, the cells were treated with free CUR, FAP/CUR, MIX/CUR and FBP/CUR micelles at different concentrations ranging from 3.125 μM to 100 μM, respectively. The cells treated with blank FAP, FBP and mixed micelles at same dose of polymer concentration were investigated for the cytotoxicity of polymers. After incubation 24 h and 48 h at 37 °C, the medium solution which contained MTT (1 mg mL^{-1}) was added to each well for replaced the old medium. After 4 h incubation, the medium solution contained MTT was discarded before adding 100 μL DMSO to dissolve the formazan crystals. The optical absorbance values were measured by microplate reader at 570 nm. The experiments were repeated in triplicate.

2.14 Apoptosis assay

Bound by phosphatidylserine (PS) that was exposed on the outer leaflet, apoptotic cells were identified by FITC-labeled Annexin-V. And the cells with damaged membrane could be stained with PI. Thus, apoptotic cells which were induced by different treatments were quantified by flow cytometric with Annexin V-FITC/PI double staining.[37] Hepa1-6 and SMMC-7721 cells (200 000 per well) were placed in 6-well plates and incubated overnight, then the cells were treated with FAP/CUR, FBP/CUR, MIX/CUR and free CUR (equivalent concentration of 50 μM CUR for SMMC-7721 cells and 25 μM CUR for Hepa1-6 cells). 24 h later, the cells were collected and centrifuged, then washed with PBS. The precipitations were suspended in 500 μL binding buffer (Annexin V-FITC 5.0 μL) and stained in dark for 15 min. Finally, 2.0 μL PI solution was added and evaluated on the flow cytometer (FCM, BD Ltd, USA).

2.15 Morphological apoptosis detection

Cellomics array scan VTI 600 (HCS reader, Thermo Fisher Scientific, USA) was used to observe the morphological changes in nucleus after staining with Hoechst 33342. Hepa1-6 and SMMC-7721 cells (8000 per well) were placed in 96-well plate in 100 μL DMEM medium which containing 10% FBS. After incubation overnight, the cells were treated with free CUR, FAP/CUR, MIX/CUR and FBP/CUR micelles (equivalent concentration of 50 μM CUR for SMMC-7721 cells and 25 μM CUR for Hepa1-6 cells). 6 h later, cells were washed with PBS and fixed with 4% paraformaldehyde (PFA) for 10 min at room

temperature. Fixed cells were washed with PBS and stained with Hoechst 33342 (5 μg mL^{-1}) for 10 min in dark environment before testing.

2.16 Cellular uptake assay

In order to study the cellular internalization of mixed micelles, nile red labeled micelles (MIX/NR) were prepared by the thin film hydration method mentioned above in 2.6. Hepa1-6 and SMMC-7721 cells (8000 per well) were placed in 96-well plates with 100 μL DMEM medium and incubated overnight. Then the medium was replaced by novel medium which containing NR solution or NR loaded micelles (5 μM) for 1 h, 3 h and 6 h, respectively. The cells were washed with PBS three times, and 1 mL 4% PFA was added to fix the cells for 10 min later. Then the PFA was replaced by 1 mL Hoechst 33342 (10 μg mL^{-1}) and stained for 10 min. The fluorescence intensity of each well was measured by HCS reader with excitation wave-length at 480 nm and emission wave-length at 578 nm.

At the same time, cellular uptake was also assayed by FCM. Hepa1-6 and SMMC-7721 cells (100 000 per well) were placed in 12-well plates and incubated overnight. Then the medium was replaced by novel medium which containing NR solution or NR loaded micelles (5 μM) for 1 h, 3 h and 6 h, respectively. After removing medium, the cells were washed with PBS three times. The cells were collected and centrifuged. The precipitations were suspended in PBS for detection with FCM.

2.17 CUR loaded micelles induce reactive oxygen species (ROS) generation

A power of studies manifested that ROS level increase has closely knitted with cancer cell death.[38] Intracellular ROS generation was detected by 2′,7′-dichlorodihydrofluorescein diacetate (DCFH-DA) staining. DCFH-DA could pass the membrane into the cells and be cleaved by esterase inside the cells to form 2′,7′-dichlorodihydrofluorescein (DCFH), which was further oxidized by ROS to form dichlorofluorescein (DCF) which has green fluorescence.[38] In short words, Hepa1-6 and SMMC-7721 cells (8000 per well) were placed in 96-well plate in 100 μL DMEM medium and incubated overnight. The cells were treated with free CUR, FBP/CUR, FAP/CUR and MIX/CUR micelles (equivalent concentration of 50 μM CUR for SMMC-7721 cells and 25 μM CUR for Hepa1-6 cells), respectively. 6 h later, the cells were washed twice by PBS, and stained with DCFH-DA (10 μM) at 37 °C for 30 min. The stained cells were washed with FBS for twice. The intensity of green fluorescence reflected the intracellular ROS was measured by microplate reader with an excitation wavelength of 485 nm and the emission wavelength of 538 nm.

2.18 Statistical analysis

All quantitative data is expressed as mean ± SD, $n = 3$. The statistical analysis was done by GraphPad Prism 5 and Origin 8.0 software. Statistical comparison was analyzed by *t*-test. $P < 0.05$ was considered as statistically significant.

3 Result

3.1 Characterization of FAP and FGA conjugate

A novel amphiphilic FAP polymer was synthesized *via* the esterification and electrophilic addition reaction (Fig. 2A). The FGA polymer was synthesized *via* the esterification (Fig. 2B). ^{1}H-NMR and FTIR spectra were used to display the structures of raw materials, FAP and FGA. Fig. 3A showed the ^{1}H-NMR spectra of PCL, PCL–CH=CH_2, F68, GA, FGA and FAP, respectively. The ^{1}H-NMR spectra of PCL and PCL–CH=CH_2 showed the characteristic peaks of PCL, including e ($\delta = 1.29$ ppm), c and d ($\delta = 1.57$ ppm), b ($\delta = 2.25$ ppm) and a ($\delta = 4.08$ ppm). Furthermore, the peaks, g_1 ($\delta = 2.72$ ppm), g_2 ($\delta = 3.18$ ppm) and f ($\delta = 6.65$ ppm), were belonged to the double bond group at the end of PCL–CH=CH_2. After the electrophilic addition reaction, peak f, g_1 and g_2 were disappeared in the spectrum of FAP. At the same time, the typical peaks of PCL and F68 which included peak l ($\delta = 1.37$ ppm), peak j ($\delta = 3.38$ ppm), peak k ($\delta = 3.34$ ppm) for polypropylene oxide and the peaks h and i ($\delta = 3.60$ ppm) for polyethylene oxide were appeared in the ^{1}H-NMR spectra of FAP. The emergence of these characteristic peaks in FAP spectra indicated the successful synthesis.

The peaks of q, r and s ranging from 0.8 ppm till 1.78 ppm, n ($\delta = 3.25$ ppm), p ($\delta = 2.28$ ppm), o ($\delta = 2.76$ ppm) and m ($\delta = 5.73$ ppm) were belonged to GA. In addition to above mentioned

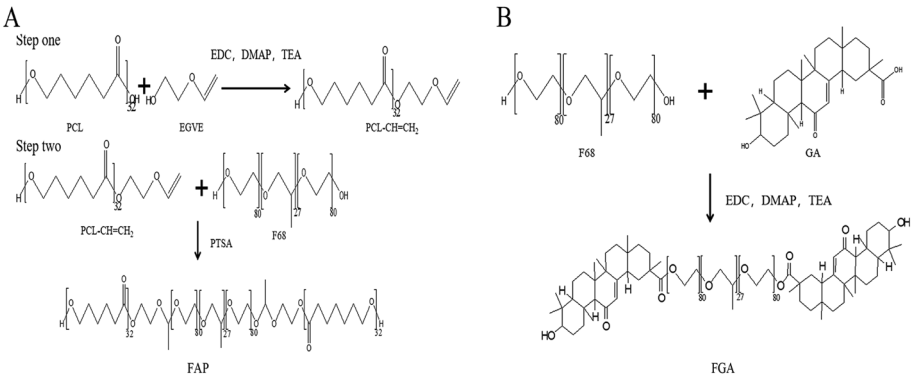

Fig. 2 The synthesis routes of FAP (A) and FGA (B).

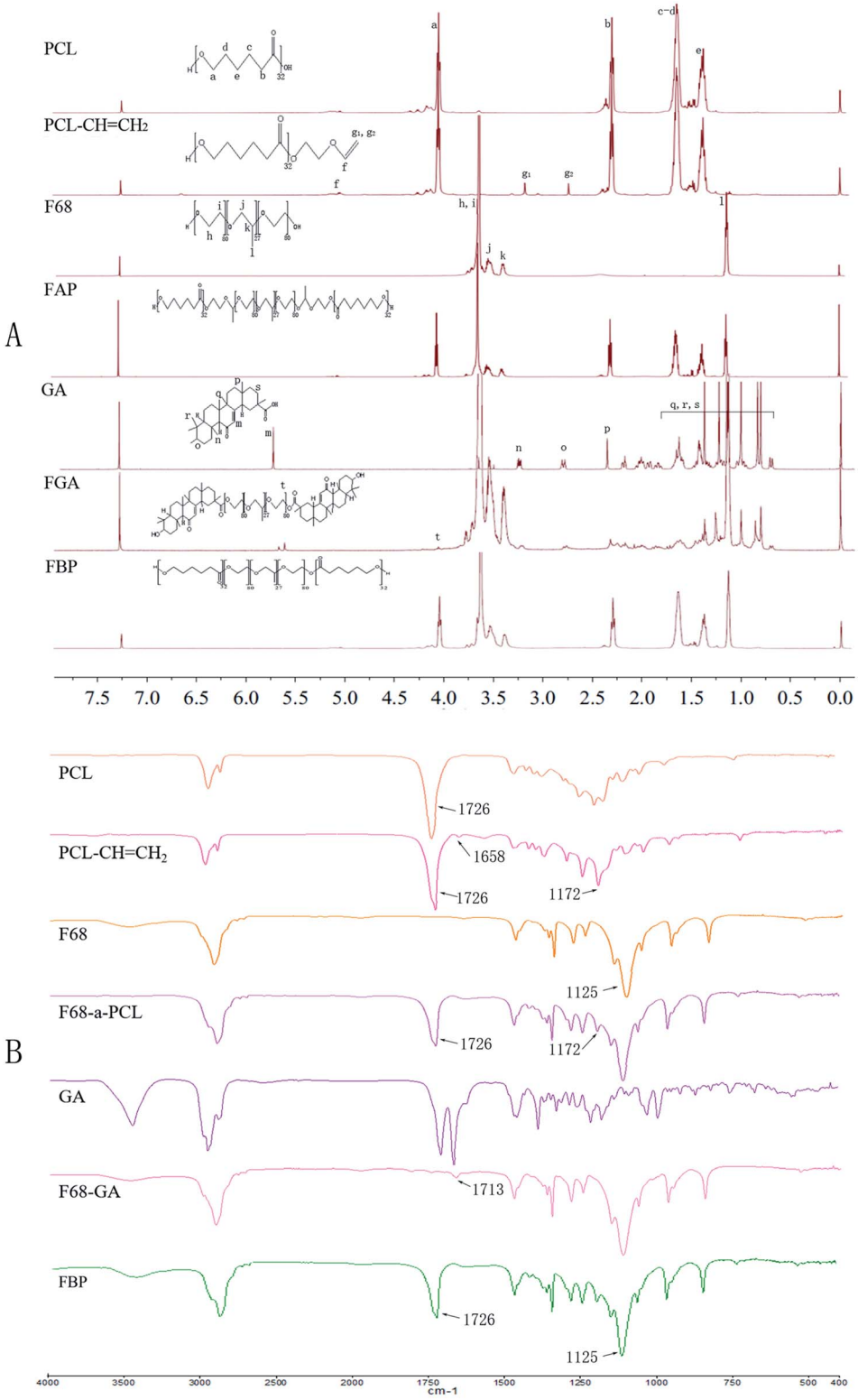

Fig. 3 The 1H-NMR (A) and FTIR (B) spectra of FAP and FGA.

peaks of F68 and GA, a new peak t ($\delta = 4.09$ ppm) was merged in the spectrum of FGA. It indicated that FGA was successfully synthesized.

Moreover, the structure of FAP and FGA polymer were verified by FTIR, the results were shown in Fig. 3B. There was a peak which associated with double bond appearing in PCL–CH=CH_2 spectrum at 1658 cm^{-1}. The peak at 1658 cm^{-1} vanished in

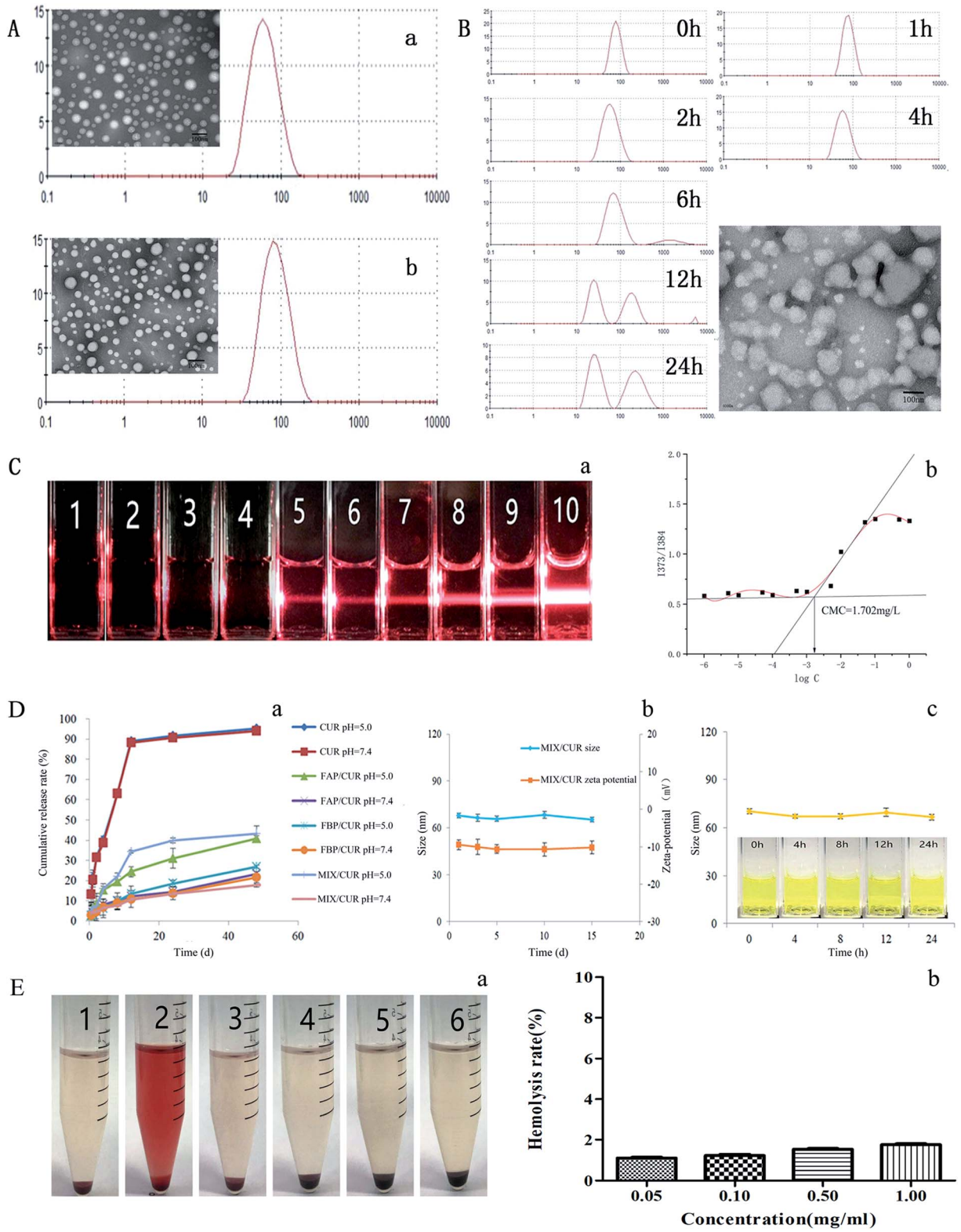

Fig. 4 Charts of formulation evaluation of mixed micelles. (A) The particle size and TEM images of mixed micelles, (a) BMM, (b) MIX/CUR, the rulers represent 100 nm; (B) the particle size changes of the MIX/CUR micelles and the TEM image of MIX/CUR micelles under weakly acid environment for 24 h; (C) the result of CMC and Tyndall phenomenon, (a) photos of mixed micellar solutions with the irradiation of red laser at various concentrations: 1. PBS, 2. 1.0×10^{-4} mg mL^{-1}, 3. 5.0×10^{-4} mg mL^{-1}, 4. 1.0×10^{-3} mg mL^{-1}, 5. 5.0×10^{-3} mg mL^{-1}, 6. 1.0×10^{-2} mg mL^{-1}, 7. 5.0×10^{-2} mg mL^{-1}, 8. 1.0×10^{-1} mg mL^{-1}, 9. 5.0×10^{-1} mg mL^{-1}, 10. 1.0 mg mL^{-1}, (b) the CMC of the mixed micelles; (D) CUR cumulative release profiles and the stability of MIX/CUR micelles, (a) the profiles of cumulative release, (b) the particle size and zeta potential of MIX/CUR during the storage period, (c) the stability of MIX/CUR micelles and the apparent character of MIX/CUR micelles in PBS containing 10% FBS for 24 h; (E) the results of hemolysis assay. (a) The hemolysis situation of BMM in different concentrations. (1) Negative control group, (2) positive control group, (3) BMM at 1.00 mg mL^{-1}, (4) BMM at 0.50 mg mL^{-1}, (5) BMM at 0.10 mg mL^{-1}, (6) BMM at 0.05 mg mL; (b) the bar chart of hemolysis rate of BMM in various concentrations ($n = 3$).

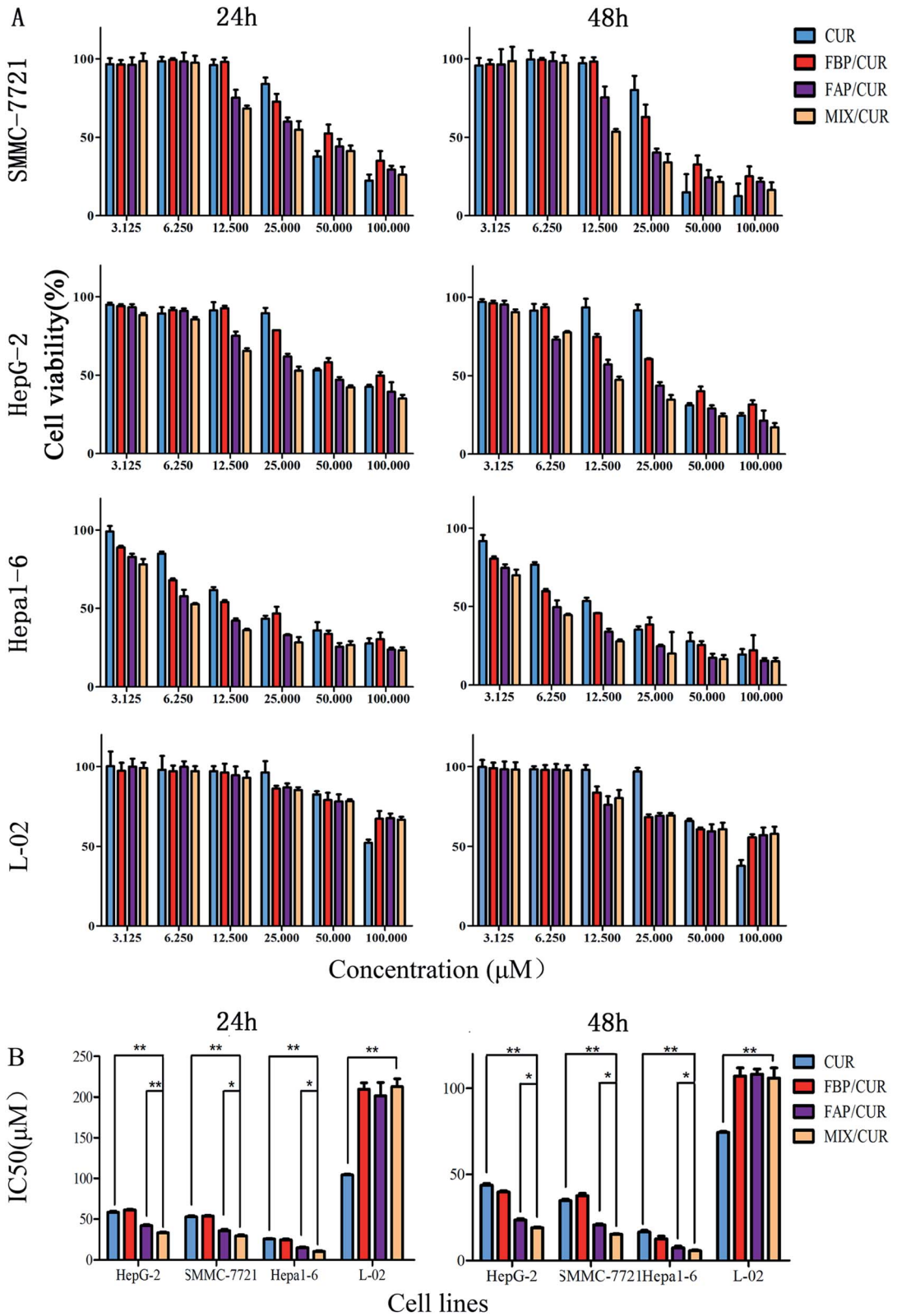

Fig. 5 The cell viability (A) and IC_{50} (B) of SMMC 7721, Hepa1-6, HepG2, and L-02 cells which were treated with free CUR and CUR loaded micelles for 24 h and 48 h. *$P < 0.05$, **$P < 0.01$.

spectrum and a new peak which belonged to F68 arisen at 1172 cm^{-1}. The arising and vanishing of these peaks in FAP spectra showed that FAP was successfully synthesized. The vibration peak of the ester bond which was formed by the carboxyl group in GA and the hydroxyl group in F68 was arisen at 1713 cm^{-1}. It indicated that FGA was successfully synthesized.

3.2 Characterization of MIX/CUR micelles

To understand the characteristics of MIX/CUR micelles, the morphology, zeta potential, particle size, DL and EE were evaluated in this study. The particle sizes of blank micelles and drug loaded micelles were tested by DLS, and the mean diameters were 68.11 ± 1.53 nm and 91.06 ± 1.37 nm, respectively (Fig. 4A). Both of them had narrow size distribution (PDI = 0.193 ± 0.020 for MIX/CUR micelles and PDI = 0.187 ± 0.013 for BMM). The zeta potential of −9.79 ± 0.47 mV for the MIX/CUR micelles was observed in this study.

The TEM images showed that MIX/CUR micelles were spherical shapes, homogeneous and smooth edges without aggregation (Fig. 4A), which demonstrated that the micelles preserved the completion of the structure. The diameters of MIX/CUR micelles which obtained by the TEM images were well fitted with the size were measured by DLS. The DL and EE of MIX/CUR micelles measured by HPLC were 6.31% ± 0.92% and 75.13% ± 1.36%, respectively.

3.3 pH-responsive degradation of micelles

The acid-labile acetal linker between PCL and F68 made micelles susceptible to disassemble under weakly acid condition. The particle size change of MIX/CUR micelles under the weakly acid condition were monitored by DLS. After incubation at pH = 5.0 for 6 h, particle size changes of the micelles were detected (Fig. 4B). Small particles and large aggregates were also observed (Fig. 4B).

3.4 CMC

The anti-dilution ability of mixed micelles was estimated by classic Tyndall effect. As shown in Fig. 4C-a, when the concentration of BMM were 1.0×10^{-4} mg mL^{-1} to 1.0 mg mL^{-1}, under the red laser irradiation, blank mixed micellar solutions presented a clear light beam when the micelle concentration was above 5.0 mg L^{-1} (Fig. 4C-a, sample 5). As shown in Fig. 4C-b, the CMC value of mixed micelles was 1.702 mg L^{-1}, it was lower than F68.[20]

3.5 *In vitro* release of CUR from micelles

The dialysis method was utilized to investigate the *in vitro* drug release behaviors of free CUR, FBP/CUR, FAP/CUR and MIX/CUR micelles under sink conditions. As shown in Fig. 4D-a, free CUR group showed rapid release behavior that approximately 90% CUR were released in 12 h, no matter what the pH value was. At the same time, CUR loaded micelles showed sustained release profiles. Particularly, the release profile of CUR from FBP/CUR micelles were slowly and had no significant difference between weakly acid environment (pH 5.0) and physiological environment (pH 7.4).

3.6 The stability of micelles

For pharmaceutical formulations, storage stability is very important. As shown in Fig. 4D-b, negligible variations were observed for MIX/CUR micelles, indicated that it possessed excellent long-term storage stability.

As shown in Fig. 4D-c, the particle size of MIX/CUR micelles in PBS contained 10% FBS was stable without sharp changes until 24 h. Besides, the particles had no visible particle precipitation for 24 h, which showed great dispersion under this condition.

3.7 Hemolysis assay

Hemolysis plays such an essential role to evaluate the biocompatibility of materials. The hemolysis assay was performed by the method reported in the previous report.[36] Even at the concentration of 1.00 mg mL^{-1}, the BMM did not display hemolysis (Fig. 4E-a). The hemolysis rates of various concentrations of BMM were showed in Fig. 4E-b. The hemolysis rates of four groups were not beyond 2% and did not have significant difference.

3.8 Cytotoxicity assay

The survival rates of SMMC-7721, Hepa1-6, HepG-2, and L-02 cells treated with 480 μg mL^{-1} of BMM for 48 h were 91.6%, 89.3%, 93.7%, and 92.4%, respectively, which indicated that BMM have no remarkable toxicity in SMMC-7721, Hepa1-6, HepG-2, and L-02 cells. For another, when the concentrations and treatment periods increased, the cell viabilities were decreased (Fig. 5A). Displayed concentration-dependent and time-dependent inhibitory effects in SMMC-7721, Hepa1-6, HepG-2, and L-02 cells, respectively.

In SMMC-7721, HepG-2, Hepa1-6, and L-02 cells, the half maximal inhibitory concentration (IC_{50}) values of MIX/CUR,

Table 1 The IC_{50} values of three kinds of different cell lines treated with MIX/CUR, FAP/CUR, FBP/CUR and free CUR for 24 h and 48 h (mean ± SD, $n = 3$)

		IC_{50} value (μM)			
Cell line	Time (h)	CUR	FBP/CUR	FAP/CUR	MIX/CUR
HepG-2	24	59.76 ± 1.11	60.93 ± 0.64	40.51 ± 1.35	33.37 ± 0.79
	48	44.53 ± 0.94	39.38 ± 0.73	24.02 ± 0.79	18.42 ± 0.52
SMMC-7721	24	52.13 ± 1.37	53.19 ± 0.66	36.12 ± 1.55	30.53 ± 1.00
	48	34.40 ± 0.78	38.29 ± 1.28	20.39 ± 0.65	15.14 ± 0.26
Hepa1-6	24	25.79 ± 0.58	24.18 ± 1.18	15.11 ± 0.82	10.52 ± 0.86
	48	17.22 ± 1.02	12.73 ± 1.43	7.35 ± 0.90	5.75 ± 0.42
L-02	24	104.43 ± 0.96	209.42 ± 1.77	201.18 ± 3.15	212.67 ± 2.56
	48	74.60 ± 2.57	107.21 ± 1.68	108.13 ± 3.02	105.92 ± 0.93

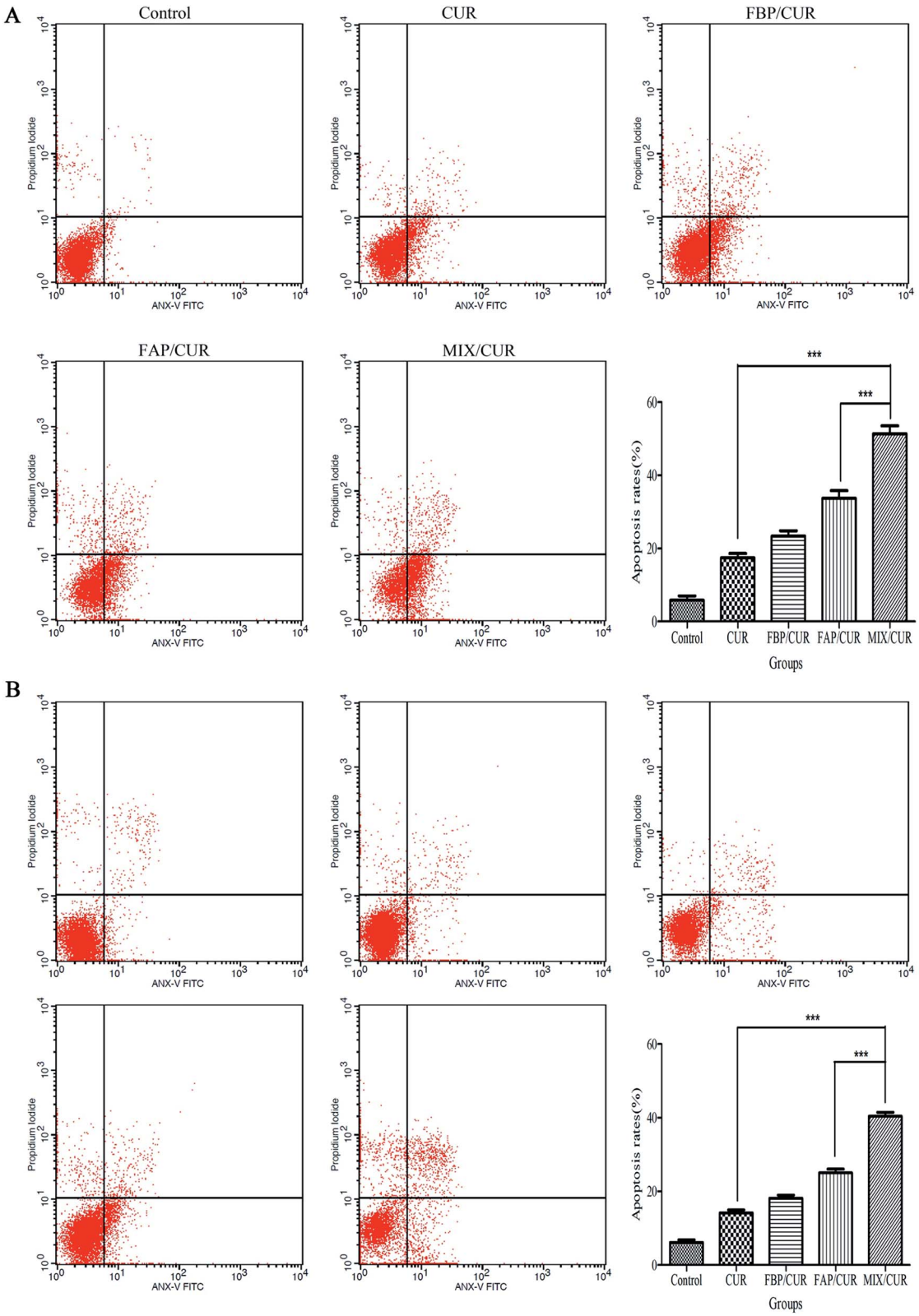

Fig. 6 The apoptosis rates of Hepa1-6 (A) and SMMC-7721 (B) cells treated with free CUR and CUR loaded micelles at the concentration of 25 μM and 50 μM CUR for 24 h. ***$P < 0.001$.

FAP/CUR, FBP/CUR and free CUR for 24 h and 48 h were showed in Table 1. It showed that the IC_{50} of MIX/CUR micelles were significantly lower than free CUR, FBP/CUR micelles and FAP/CUR micelles in HCC (Fig. 5B). However, in L-02 cells, the IC_{50} of MIX/CUR micelles was higher than free CUR and without remarkable difference with FBP/CUR micelles and FAP/CUR

micelles. The results indicated the following two points: first, MIX/CUR, FAP/CUR, FBP/CUR and free CUR had lower cytotoxicity on non-cancer cells, and higher cytotoxicity on HCC; Second, the MIX/CUR micelles modified by GA has a superior inhibitory effect on HCC.

3.9 Apoptosis assay

Cellular apoptosis was performed by Annexin V/PI staining kit according to the manufacturers' instructions. As shown in Fig. 6, few apoptosis Hepa1-6 and SMMC-7721 cells were identified in control group. Treatment with 25 μM or 50 μM free CUR, FBP/CUR, FAP/CUR and MIX/CUR micelles for 24 h significantly increased the population of apoptotic cells in Hepa1-6 or SMMC-7721 cells, respectively, with an apoptotic rate of approximately 51.38 ± 3.67% and 40.42 ± 1.86% for MIX/CUR group compared with 17.44 ± 2.09% and 14.13 ± 1.34% for free CUR-treated groups in Hepa1-6 and SMMC-7721 cells.

3.10 Morphological apoptosis detection

After staining with Hoechst 33342, the nucleus of SMMC-7721 and Hepa1-6 cells were appeared as weak blue fluorescence. Incubated by free CUR or CUR loaded micelles, the cells images showed bright chromatin condensation and nuclear fragmentation (Fig. 7A). While a higher nuclear deformation rate was found in the MIX/CUR micelles group than in free CUR, FBP/CUR and FAP/CUR groups, it implied that MIX/CUR micelles could enhance the pro-apoptotic effect of CUR.

3.11 Intracellular reactive oxygen species (ROS) generation

So as to identify the relationship between ROS and the cytotoxicity to cancer cells, the intracellular ROS level was measured by DCFH-DA staining. As shown in Fig. 7B, the intracellular ROS generation ability of different groups in Hepa1-6 and SMMC-7721 cells were aligned from high to low as following: MIX/CUR micelles > FAP/CUR micelles > FBP/CUR micelles > free CUR > control. These data supported the notion that MIX/CUR micelles had great potential in generating ROS levels in Hepa1-6 and SMMC-7721 cells *via* active targeting and pH-sensitive functions, which might exert such an essential role in anti-cancer cells.

3.12 Cellular uptake assay

In order to investigate if the high cytotoxicity of mixed micelles was closely knitted with improving cellular uptake, the cellular uptake of mixed micelles in hepatoma cell lines were detected by flow cytometry and cellomics array scan VTI. As the results of flow cytometry showed in Fig. 8A and C, MIX/NR micelles were totally different from free NR, FBP/NR and FAP/NR micelles, which exhibited an enhanced uptake in hepatoma cells after

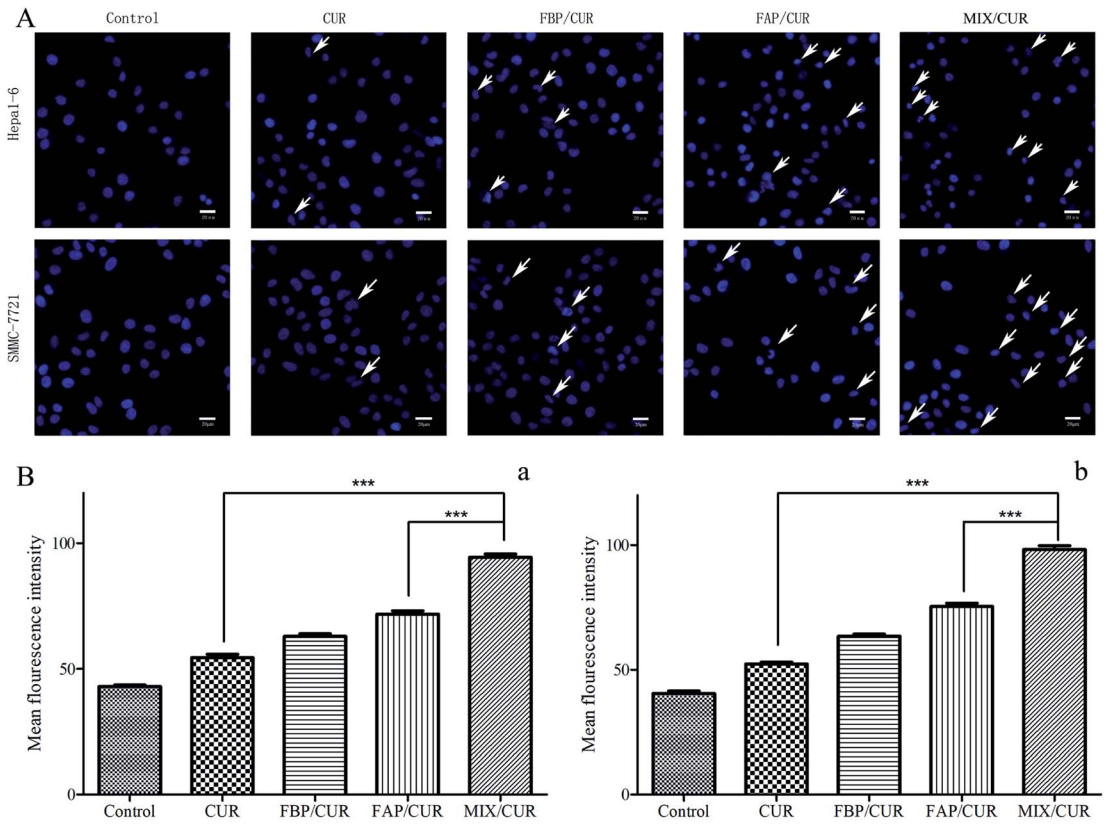

Fig. 7 Fluorescence micrographs of Hepa1-6 and SMMC-7721 cells which were incubated with free CUR and CUR loaded micelles for 8 h (A). The rulers in the graph represent 20 μm; Intracellular ROS level in Hepa1-6 (B-a) and SMMC-7721 (B-b) cells which were treated with free CUR and CUR loaded micelles at an equivalent CUR concentration for 6 h (20 μM for Hepa1-6 and 50 μM for SMMC-7721). ***$P < 0.001$.

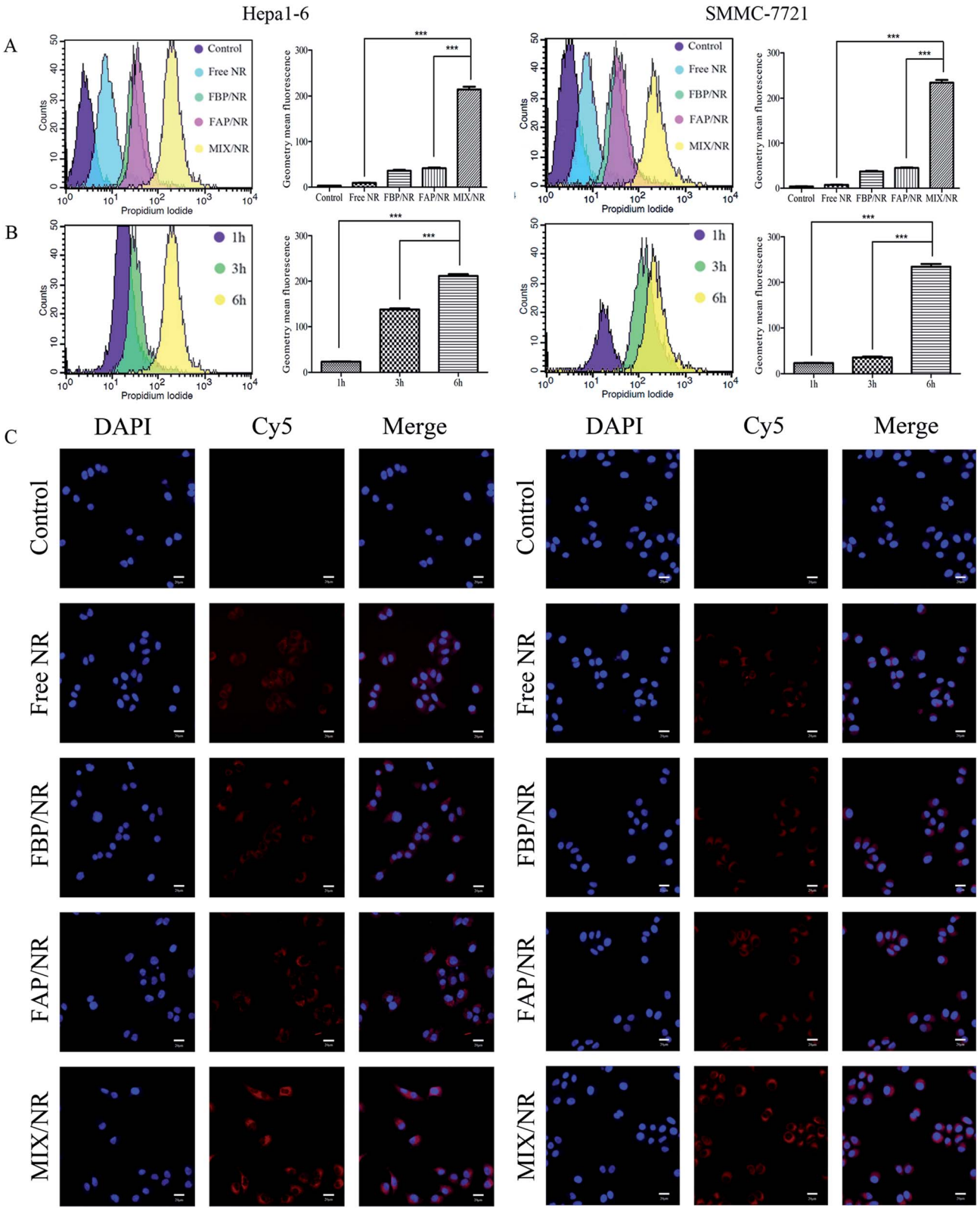

Fig. 8 The results of cellular uptake experiments. (A) Geometry mean fluorescence and histogram of fluorescence intensity the cells incubated with free NR and NR loaded micelles on Hepa1-6 and SMMC-7721 cells for 6 h; (B) geometry mean fluorescence and histogram of fluorescence intensity of the cells incubated with MIX/NR on Hepa1-6 and SMMC-7721 cells for 1 h, 3 h and 6 h, ***$P < 0.001$; (C) uptake and intracellular of free NR and NR loaded micelles. NR in cancer cells showed red fluorescence. Hoechst 33342 showed blue fluorescence. The rulers in the graph represent 20 μm.

6 h. After incubated with MIX/NR micelles for different time, the fluorescence intensity of NR of intercellular accumulation displayed time-dependent manner in Hepa1-6 and SMMC-7721 cells (Fig. 8B). The fluorescence intensity in cells that incubated with MIX/NR (NR 5 μM) was about 10-fold higher than free NR group and about 5-fold higher than FAP/NR and FBP/NR groups (Fig. 8A). The results further demonstrated that GA-modification could improve the cell uptake by GA-mediated endocytosis.

4 Discussion

In the preparation evaluations, MIX/CUR showed similarity physical–chemical properties with other research. For example, the polymer materials could form nano-size and surface negatively charged micelles. According to the previous reports, on the one hand, the high absolute value of zeta potential was closely knitted with the stability of nanoparticles.[39] On the other hand, polymer micelles with particle size within the scope of 10–200 nm could promote drug accumulation *via* enhanced permeability and retention (EPR) effect in tumor sites.[8] Therefore, the narrow size distribution and nano-size of MIX/CUR micelles might be appropriate for accumulation at the tumor site and would not be swiftly eliminated by the reticuloendothelial system.[29] Simultaneously, the DL of MIX/CUR micelles (6.31% ± 0.92%) was significantly higher than it of F68/CUR micelles (1.38%),[40] which indicated that PCL-modification could improve the DL of F68.

The *in vitro* drug release test showed that the acidic environment caused quickly drug release of FAP/CUR and MIX/CUR micelles. 48 h later, nearly 40% CUR was released at pH 5.0, while only 20% CUR was released at pH 7.4, which was similar to the results documented in other literatures.[41,42] The trend of release behaviors was fitted with pH-sensitive particle size change, it manifested that the hydrolysis of acetal linkage between F68 and PCL might led to swift drug release at weakly acidic environment. However, the particle size of MIX/CUR micelles changed when it exposed in weak acid environment for 6 h, which manifested a certain gap compared with other reports.[23,24] After the comparative analysis, the possible reason of speculation was the following one.[16] FAP was a penta-block polymer that needs to be folded when formed micelles. At this time, there might be a steric hindrance to reduce the contact between the hydrogen ion and the acetal bond, which might slow down the rate of FAP hydrolysis. It might also the reason why FAP/CUR micelles and MIX/CUR micelles displayed a sustained release behavior in drug release experiments.

The changes of CMC value might closely knitted with the proportion of hydrophobic *vs.* hydrophilic.[43] In this study, the CMC value was obviously decreased by PCL modification. It was consistent with the results of the CMC value decrease of F68 after the hydrophobic segment modification in other reports.[4,20,23] It could be speculated that increased the length of the hydrophobic chain in the amphiphilic compound might be helpful in reduced the CMC value. However, it was not sure if the ratio of the hydrophilic *vs.* hydrophobic has the best value, which had not been reported in the literatures. Besides, the Tyndall phenomenon and the CMC value could mutually verified. As it mentioned in the articles, lower CMC values might contribute to improving the dilution resistance of the formulation in circulatory system.[44,45]

The materials, as it remarked in the American Society for Testing and Materials (ASTM F756-00, 2000), were divided into three categories in terms of the degree of hemolysis: nonhemolytic (0–2% of hemolysis), slightly hemolytic (2–5% of hemolysis) and hemolytic (>5% of hemolysis).[46] The concentration of the mixed micelles did not have hemolytic properties even it reached 1 mg mL^{-1}, which manifested the exceptional blood compatibility of BMM. Therefore, it could be regard as a potential carrier for intravenous injection.

In the cytotoxicity experiment, the order of IC_{50} from large to small was as follow: HepG-2 > SMMC-7721 > Hepa1-6. It showed that SMMC-7721 and Hepa1-6 cells were more sensitive to CUR loaded micelles. So that, the SMMC-7721 and Hepa1-6 cell lines were chosen as the cancer cell models for further research. The blank micelles group did not show significant cytotoxicity in HCC and L-02 cells, indicated that the increased cytotoxicity of the formulation was not due to the polymer materials. At the same time, when compared the IC_{50} of different micelles in HCC and L-02 cells, the results showed that MIX/CUR micelles could increase the anti-HCC effect of CUR, and could improve the safety of CUR on non-cancer cells. This might be related to increased cell uptake by micelles, which was further confirmed in cell uptake experiments. The results showed that the fluorescence intensity of the NR loaded micelles groups were significantly higher than free NR group, and the fluorescence intensity of the MIX/NR group was the highest. It might be due to the GA-mediated active targeting.[47] Compared with other active targeting CUR loaded micelles, GA-modified micelles showed similar increasing cellular uptake function in cell uptake experiment.[48]

Eventually the cellular uptake increased, FBP/CUR micelles group did not show a higher cell killing ability than free CUR. It was different from some reports, this phenomenon might be attribute to sustained drug release rate.[38] The speculation was confirmed in the FAP/CUR micelles group and the MIX/CUR micelles group. Because they were formed by FAP segments, so they can be hydrolyzed in a weakly acid environment to increase the release rate of CUR from micelles. Compared with other reports, the chemical bonds which could response the tumor microenvironment had potential in improving drug release and increasing anticancer cells ability.[49,50]

5 Conclusion

In summary, a novel pH-sensitive and actively targeting mixed micelles were successfully fabricated as the new drug delivery system for enhancing anti-HCC effect. The mixed micelles consisted of FGA and FAP polymers that mediated by GA were regarded as a promising delivery system to overcome the shortages of CUR. MIX/CUR micelles exhibited a variety of attractive properties including desirable particle size, higher drug loading, favorable acid-responsive drug release kinetics, preferably stability, improved cellular internalization and

stronger cytotoxicity. Mediated by the GA receptor interaction, GA decoration on the mixed micelles considerably enhanced the endocytic rate in Hepa1-6 and SMMC-7721 cells, thereby suppressing the tumor cell proliferation and apoptosis. Consequently, this multifunctional drug delivery system has the potential to be the promising platform for highly effective hepatic anticancer activity.

Conflicts of interest

There are no conflicts to declare.

Acknowledgements

This work was supported by the National Natural Science Foundation of China under grant no. 81803743; the Fundamental Research Funds for the Central public welfare research institutes under grant no. ZXKT17006, no. ZXKT17050; Science and Technology Project of Guangxi Zhuang Autonomous Region under grant no. AA17204090 and no. AD16380013; The Basic Research Foundation of the China Academy of Chinese Medical Sciences under grant no. ZZ13-YQ-041.

References

1 Y. Eso and H. Marusawa, *Hepatol. Res.*, 2018, **48**, 597–607.
2 European Association for the Study of the Liver, *J. Hepatol.*, 2018, **69**, 182–236.
3 W. Ni, Z. Li, Z. Liu, Y. Ji, L. Wu, S. Sun, X. Jian and X. Gao, *J. Pharm. Sci.*, 2019, **108**, 1284–1295.
4 X. B. Fang, J. M. Zhang, X. Xie, D. Liu, C. W. He, J. B. Wan and M. W. Chen, *Int. J. Pharm.*, 2016, **502**, 28–37.
5 A. M. Alizadeh, M. Sadeghizadeh, F. Najafi, S. K. Ardestani, V. Erfani-Moghadam, M. Khaniki, A. Rezaei, M. Zamani, S. Khodayari, H. Khodayari and M. A. Mohagheghi, *BioMed Res. Int.*, 2015, **2015**, 824746.
6 H. Y. Zhang, C. Y. Sun, M. Adu-Frimpong, J. N. Yu and X. M. Xu, *Int. J. Pharm.*, 2019, **555**, 270–279.
7 P. R. Sarika, N. R. James, P. R. Kumar and D. K. Raj, *Int. J. Biol. Macromol.*, 2016, **86**, 1–9.
8 M. Gou, K. Men, H. Shi, M. Xiang, J. Zhang, J. Song, J. Long, Y. Wan, F. Luo, X. Zhao and Z. Qian, *Nanoscale*, 2011, **3**, 1558–1567.
9 Z. D. Lv, X. P. Liu, W. J. Zhao, Q. Dong, F. N. Li, H. B. Wang and B. Kong, *Int. J. Clin. Exp. Pathol.*, 2014, **7**, 2818–2824.
10 J. Ma, B. Fang, F. Zeng, H. Pang, J. Zhang, Y. Shi, X. Wu, L. Cheng, C. Ma, J. Xia and Z. Wang, *Toxicol. Lett.*, 2014, **231**, 82–91.
11 R. Feng, W. Zhu, W. Chu, F. Teng, N. Meng, P. Deng and Z. Song, *Anti-Cancer Agents Med. Chem.*, 2017, **17**, 599–607.
12 A. B. Kunnumakkara, D. Bordoloi, C. Harsha, K. Banik, S. C. Gupta and B. B. Aggarwal, *Clin. Sci.*, 2017, **131**, 1781–1799.
13 E. Willenbacher, S. Z. Khan, S. C. A. Mujica, D. Trapani, S. Hussain, D. Wolf, W. Willenbacher, G. Spizzo and A. Seeber, *Int. J. Mol. Sci.*, 2019, **20**, DOI: 10.3390/ijms20081808.
14 M. A. Tomeh, R. Hadianamrei and X. Zhao, *Int. J. Mol. Sci.*, 2019, **20**, DOI: 10.3390/ijms20051033.
15 K. Wang, C. Guo, S. Zou, Y. Yu, X. Fan, B. Wang, M. Liu, L. Fang and D. Chen, *Artif. Cells, Nanomed., Biotechnol.*, 2018, **46**, 659–667.
16 P. Kumari, S. V. K. Rompicharla, O. S. Muddineti, B. Ghosh and S. Biswas, *Int. J. Biol. Macromol.*, 2018, **116**, 1196–1213.
17 T. Yan, D. Li, J. Li, F. Cheng, J. Cheng, Y. Huang and J. He, *Colloids Surf., B*, 2016, **145**, 526–538.
18 P. R. Sarika, N. R. James, P. R. Kumar, D. K. Raj and T. V. Kumary, *Carbohydr. Polym.*, 2015, **134**, 167–174.
19 V. Tzankova, C. Gorinova, M. Kondeva-Burdina, R. Simeonova, S. Philipov, S. Konstantinov, P. Petrov, D. Galabov and K. Yoncheva, *Food Chem. Toxicol.*, 2016, **97**, 1–10.
20 Y. Song, Q. Tian, Z. Huang, D. Fan, Z. She, X. Liu, X. Cheng, B. Yu and Y. Deng, *Int. J. Nanomed.*, 2014, **9**, 2307–2317.
21 M. H. Cha, J. Choi, B. G. Choi, K. Park, I. H. Kim, B. Jeong and D. K. Han, *J. Colloid Interface Sci.*, 2011, **360**, 78–85.
22 S. S. Kulthe, N. N. Inamdar, Y. M. Choudhari, S. M. Shirolikar, L. C. Borde and V. K. Mourya, *Colloids Surf., B*, 2011, **88**, 691–696.
23 Y. Cai, S. Wang, M. Wu, J. K. Tsosie, X. Xie, J. Wan, C. He, H. Tian, X. Chen and M. Chen, *RSC Adv.*, 2016, **6**, 35318–35327.
24 Y. Liu, Y. Xu, M. Wu, L. Fan, C. He, J. B. Wan, P. Li, M. Chen and H. Li, *Int. J. Nanomed.*, 2016, **11**, 3167–3178.
25 N. V. Cuong, M. F. Hsieh, Y. T. Chen and I. Liau, *J. Biomater. Sci., Polym. Ed.*, 2011, **22**, 1409–1426.
26 L. B. Macedo, D. R. Nogueira-Librelotto, J. de Vargas, L. E. Scheeren, M. P. Vinardell and C. M. B. Rolim, *AAPS PharmSciTech*, 2019, **20**, 165.
27 K. Men, M. L. Gou, Q. F. Guo, X. H. Wang, S. Shi, B. Kan, M. J. Huang, F. Luo, L. J. Chen, X. Zhao, Z. Y. Qian, S. F. Liang and Y. Q. Wei, *J. Nanosci. Nanotechnol.*, 2010, **10**, 7958–7964.
28 T. Wang, M. Li, H. Gao and Y. Wu, *J. Colloid Interface Sci.*, 2011, **353**, 107–115.
29 J. Zhang, R. Chen, X. Fang, F. Chen, Y. Wang and M. Chen, *Nano Res.*, 2015, **8**, 201–218.
30 S. Aryal, C. M. Hu and L. Zhang, *ACS Nano*, 2010, **4**, 251–258.
31 M. Chang, M. Wu and H. Li, *Drug Delivery*, 2018, **25**, 1984–1995.
32 H. Singh, S. J. Kim, D. H. Kang, H. R. Kim, A. Sharma, W. Y. Kim, C. Kang and J. S. Kim, *Chem. Commun.*, 2018, **54**, 12353–12356.
33 H. Singh, J. Y. Lim, A. Sharma, D. W. Yoon, J. H. Kim, Z. Yang, J. Qu, J. Kim, S. G. Lee and J. S. Kim, *ChemBioChem*, 2019, **20**, 614–620.
34 T. Yang, Y. Lan, M. Cao, X. Ma, A. Cao, Y. Sun, J. Yang, L. Li and Y. Liu, *Colloids Surf., B*, 2019, **175**, 106–115.
35 Y. Zheng, S. Shi, Y. Liu, Y. Zhao and Y. Sun, *J. Biomater. Appl.*, 2019, **34**, 141–151.
36 S. Liu, W. Huang, M. J. Jin, B. Fan, G. M. Xia and Z. G. Gao, *Eur. J. Pharm. Sci.*, 2016, **82**, 171–182.

37 H. Yang, N. Wang, L. Mo, M. Wu, R. Yang, X. Xu, Y. Huang, J. Lin, L. M. Zhang and X. Jiang, *Mater. Sci. Eng., C*, 2019, **98**, 9–18.
38 Y. Liu, L. Lin, J. Song, Y. Zhao, Z. Chao and H. Li, *RSC Adv.*, 2017, **7**, 47091–47098.
39 W. Hong, H. Shi, M. Qiao, Z. Zhang, W. Yang, L. Dong, F. Xie, C. Zhao and L. Kang, *Sci. Rep.*, 2017, **7**, 42465.
40 A. Sahu, N. Kasoju, P. Goswami and U. Bora, *J. Biomater. Appl.*, 2010, **25**, 619–639.
41 Q. T. Phan, M. H. Le, T. T. Le, T. H. Tran, P. N. Xuan and P. T. Ha, *Int. J. Pharm.*, 2016, **507**, 32–40.
42 T. Jabri, M. Imran, A. Aziz, K. Rao, M. Kawish, M. Irfan, M. I. Malik, S. U. Simjee, M. Arfan and M. R. Shah, *Drug Dev. Ind. Pharm.*, 2019, **45**, 703–714.
43 I. E. Klosowska-Chomiczewska, K. Medrzycka, E. Hallmann, E. Karpenko, T. Pokynbroda, A. Macierzanka and C. Jungnickel, *J. Colloid Interface Sci.*, 2017, **488**, 10–19.
44 M. Jones and J. Leroux, *Eur. J. Pharm. Biopharm.*, 1999, **48**, 101–111.
45 J. Xu, X. Zhang, Y. Chen, Y. Huang, P. Wang, Y. Wei, X. Ma and S. Li, *Mol. Pharmaceutics*, 2017, **14**, 31–41.
46 F. K. Andrade, J. P. Silva, M. Carvalho, E. M. Castanheira, R. Soares and M. Gama, *J. Biomed. Mater. Res., Part A*, 2011, **98**, 554–566.
47 J. Li, H. Xu, X. Ke and J. Tian, *J. Drug Targeting*, 2012, **20**, 467–473.
48 L. Huang, M. Cai, X. Xie, Y. Chen and X. Luo, *J. Biomater. Sci., Polym. Ed.*, 2014, **25**, 1407–1424.
49 L. Bu, H. Zhang, K. Xu, B. Du, C. Zhu and Y. Li, *Drug Delivery*, 2019, **26**, 300–308.
50 Y. Li, A. Yu, L. Li and G. Zhai, *J. Drug Targeting*, 2018, **26**, 753–765.